

Coagulation under Flow: The Influence of Flow-Mediated Transport on the Initiation and Inhibition of Coagulation

Aaron L. Fogelson^{a, b} Nesy Tania^a

Departments of ^aMathematics and ^bBioengineering, University of Utah, Salt Lake City, Utah, USA

Key Words

Coagulation · Mathematical model · Flow · Transport · Threshold · Tissue factor · TFPI · APC · Platelet deposition

Abstract

A mathematical model of intravascular coagulation is presented; it encompasses the biochemistry of the tissue factor pathway, platelet activation and deposition on the subendothelium, and flow- and diffusion-mediated transport of coagulation proteins and platelets. Simulation experiments carried out with the model indicate the predominant role played by the *physical* processes of platelet deposition and flow-mediated removal of enzymes in inhibiting coagulation in the vicinity of vascular injury. Sufficiently rapid production of factors IXa and Xa by the TF:VIIa complex can overcome this inhibition and lead to formation of significant amounts of the tenase complex on the surface of activated platelets and, as a consequence, to substantial thrombin production. Chemical inhibitors are seen to play almost no (TFPI) or little (AT-III and APC) role in determining whether substantial thrombin production will occur. The role of APC is limited by the necessity for diffusion of thrombin from the site of injury to nearby endothelial cells to form the thrombomodulin-thrombin complex and for diffusion in

the reverse direction of the APC made by this complex. TFPI plays an insignificant part in inhibiting the TF:VIIa complex under the conditions studied whether its action involves sequential binding of TFPI to Xa and then TFPI: Xa to TF:VIIa, or direct binding of TFPI to Xa already bound to the TF:VIIa complex.

Copyright © 2005 S. Karger AG, Basel

1 Introduction

Intravascular production of the key coagulation enzyme thrombin involves a complex biochemical network coordinated with activation and deposition of platelets on the vessel wall, and, importantly, occurs under flow. The influences of platelet deposition and flow on the coagulation process are seldom considered either experimentally or in mathematical models, but potentially have a strong impact on eventual thrombin production. In this paper, we build on our previous modeling efforts [1] involving the interactions of coagulation, platelet deposition, and flow-mediated transport to explore the impact of flow on early coagulation events, and on the effectiveness of the coagulation inhibitors tissue factor pathway inhibitor (TFPI) and activated protein C (APC) at a site of injury-induced thrombosis.

Below we describe the components of the models, review the salient results described in [1], and present extensions of the earlier model to incorporate the chemistry of the APC pathway on endothelial cells (ECs) adjacent to the injury, and the transport of thrombin and APC between the injury and these ECs. We also describe modeling of two variants of the TFPI pathway and explore their effectiveness.

Experiments done in the absence of flow suggest that inhibition by TFPI and antithrombin-III (AT-III) is the primary obstacle to tissue factor (TF)-initiated coagulation, and that a level of TF:VIIa complex formation sufficient to overcome this inhibition leads to substantial thrombin production [2]. In contrast, our simulations of coagulation under flow suggest that the main determinant of whether substantial thrombin production occurs is the competition between factor IXa and Xa activation by TF:VIIa on the subendothelium and the removal of these factors by flow. In our model, TF:VIIa activity decreases and finally ceases as the subendothelium becomes covered by adherent platelets, and so activation of IXa and Xa by TF:VIIa stops after several minutes. If, by this time, factor Xa has activated sufficient platelet-bound VIIIa to serve as cofactor for TF:VIIa-activated IXa, and a significant amount of the tenase complex has formed on the platelets' surfaces, then large amounts of thrombin will be produced. If IXa and Xa activation are slow because TF expression is low, little thrombin will be produced. The simulations show that none of the chemicals thought to play a major inhibitory role in coagulation, namely, TFPI, antithrombin-III (AT-III), and APC, plays a significant role in determining thrombin production in the primary thrombus at a site of vascular injury. Rather it is competition between TF:VIIa activity and platelet deposition, and competition between diffusion of IXa and Xa from the subendothelium to the platelets' surfaces and flow-mediated removal of these factors before they reach the platelets that determines the level of thrombin that will be produced.

2 Review of Flow-Mediated Coagulation Model

We begin by sketching the components of our earlier model [1] and refer the reader to that paper for details. The model describes events in a thin layer above a small (e.g., $10 \times 10 \mu\text{m}$) vascular injury. We refer to this layer as the *reaction zone*. The height of the reaction zone is determined by the blood's flow speed and the diffusion coefficients of the coagulation proteins. It is initially ap-

proximately $1 \mu\text{m}$, but increases as platelets deposit on the injured vessel surface (see below). Within the reaction zone, we consider reactions that occur in the fluid phase as well as those that occur on the surfaces of the subendothelial matrix, activated platelets, and nearby ECs. The model involves proteins and platelets and we regard all species, fluid-phase or surface-phase, as well-mixed in the reaction zone, so that each is characterized by its (volume) concentration. The model consists of ordinary differential equations that govern the rate of change of each species' concentration according to a Mass-Action-kinetics description of the reactions in which it is involved.

We assume that flow and diffusion combine to deliver proteins and platelets into the reaction zone and to remove *unbound* species from it. The rate at which the concentration of a particular species changes as the species enters or leaves the reaction zone is modeled as $k_{\text{flow}}^c (c_{\text{out}} - c)$ where c is the species' concentration in the reaction zone, c_{out} is its concentration far outside the zone, and k_{flow}^c is the rate constant for transport. The value of $k_{\text{flow}}^c = 3/4 ((V^2 D)/(R^2 L^2))^{1/3}$ is determined by the blood flow speed V , protein diffusion coefficient D , vessel radius R , and the length L of the injury¹. For a species which is consumed in the coagulation reactions, $c_{\text{out}} > c$, so transport brings that species into the reaction zone, while for a species whose concentration in plasma is low, such as the enzymes produced during coagulation, $c_{\text{out}} < c$, and flow removes that species at the specified rate (fig. 1a).

The individual molecular species included in the model are the coagulation zymogens (factors V, VII, VIII, IX, X, prothrombin); the corresponding enzymes or activated cofactors (Va, VIIa, VIIIa, IXa, Xa, thrombin); inhibitors (AT-III, TFPI, APC), and binding sites on the subendothelial surface (TF), the platelet surface ($P_5, P_8, P_9, P_9^*, P_{10}, P_2$), and the endothelium (TM). Here, TF refers to tissue factor, TM to thrombomodulin, and P_5, P_8, P_9, P_{10} , and P_2 to specific protein binding sites on the surface of activated platelets for the respective zymogen/enzyme pairs V/Va, VIII/VIIIa, IX/IXa, X/Xa, and prothrombin and thrombin. P_9^* refers to binding sites on the activated platelet surface to which only the activated factor IXa can bind. The platelet surface binding sites are assumed to be accessible only on the surfaces of activated platelets, so their concentrations are up-regulated when platelets are activated (see below).

¹ V is the mid-lumen flow velocity and is related to the wall shear rate γ by $\gamma = 2V/R$. The velocity a small distance h from the vessel wall is $\gamma \cdot h$.

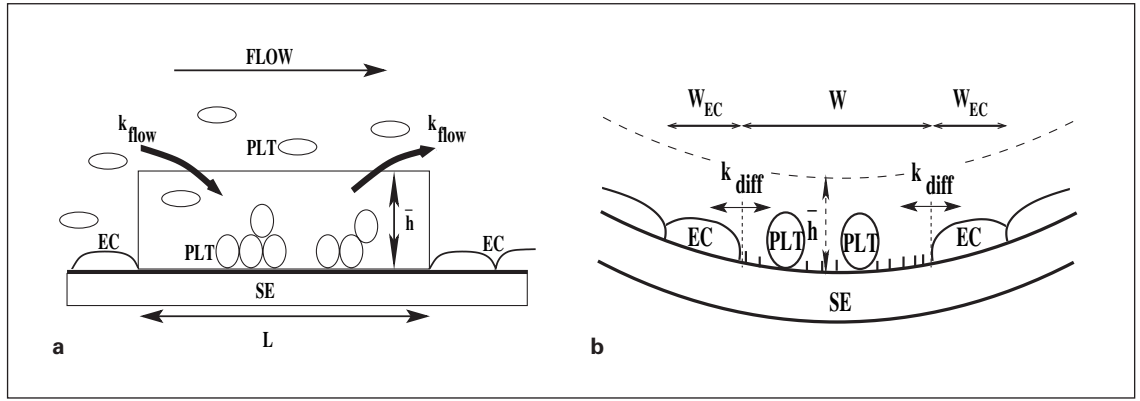


Fig. 1. a Side view of the reaction zone in which thrombin is produced. **b** Cross-section of reaction zone and adjacent endothelial zone. The flow direction is out of the paper towards the reader.

Within the model, a particular protein may appear in several forms, e.g., factor Xa can be free in the fluid and not bound to anything, in the fluid and bound to TFPI, bound to VII or the TF:VII complex (on the way to activating VII), bound to its specific binding site (P_{10}) on a platelet's surface, bound also to factor Va on a platelet's surface to form prothrombinase, and bound in transient complexes with factors V or VIII on the platelet's surface on the way to activating these cofactors and then unbinding from them. The equations governing the dynamics of the concentration (e_{10}) of fluid-phase Xa and the concentration (e_{10}^m) of Xa bound to the platelet surface membrane are given below to illustrate the nature of the reactions considered in the model. In these equations, the concentration of a zymogen or enzyme is indicated, respectively, by a subscripted z or e , e.g., z_7 refers to the concentration of VII in solution. A superscript m denotes a species bound to the subendothelial matrix or platelet surface membrane, so z_7^m refers to the concentration of subendothelial-bound TF:VII and e_{10}^m is the concentration of Xa bound to its platelet binding site P_{10} . The complex of, say, VII with Xa, is denoted $Z_7 : E_{10}$ and its concentration is denoted by $[Z_7 : E_{10}]$. The notation is consistent with that used in [1].

Equation (2.1) governing the concentration of fluid-phase factor Xa has terms describing the rates at which Xa is (A) produced by the TF:VIIa complex on the sub-endothelium, (B) is transported away by flow, (C) binds to and dissociates from TFPI, (D, E) transiently binds to VII or TF:VII on the way to activating them, (F) is inactivated by AT-III, and (G) binds to and dissociates from P_{10} on the platelet surface. Here, p_{10} denotes the total concentration of P_{10} binding sites and $p_{10} - e_{10}^{m\,tot} - z_{10}^{m\,tot}$

denotes the concentration of such sites not already occupied by a Xa- or X-containing molecule.

$$\begin{aligned} \frac{de_{10}}{dt} = & \underbrace{k_8^{cat} [Z_{10} : E_7^m]}_A - \underbrace{k_{flow}^c e_{10}}_B - \underbrace{k_{10}^+ [TFPI] e_{10} + k_{10}^- [TFPI : E_{10}]}_C \\ & + \underbrace{(k_1^- + k_1^{cat}) [Z_7 : E_{10}] - k_1^+ z_7 e_{10}}_D \\ & + \underbrace{(k_2^- + k_2^{cat}) [Z_7^m : E_{10}] - k_2^+ z_7^m e_{10}}_E \\ & - \underbrace{k_{10}^{in} e_{10}}_F - \underbrace{k_{10}^{on} e_{10} (p_{10} - e_{10}^{m\,tot} - z_{10}^{m\,tot}) + k_{10}^{off} e_{10}^m}_G \end{aligned} \quad (2.1)$$

$$\begin{aligned} \frac{de_{10}^m}{dt} = & \underbrace{k_{10}^{on} e_{10} (p_{10} - e_{10}^{m\,tot} - z_{10}^{m\,tot}) - k_{10}^{off} e_{10}^m}_G \\ & + \underbrace{(k_5^- + k_5^{cat}) [Z_5^m : E_{10}] - k_5^+ z_5^m e_{10}^m}_H \\ & + \underbrace{(k_6^- + k_6^{cat}) [Z_8^m : E_{10}] - k_6^+ z_8^m e_{10}^m}_I \\ & + \underbrace{k_{pro}^- [PRO] - k_{pro}^+ e_5^m e_{10}^m}_J + \underbrace{k_4^{cat} [Z_{10}^m : TEN]}_K + \underbrace{k_4^{cat} [Z_{10}^m : TEN^*]}_L \end{aligned} \quad (2.2)$$

Equation (2.2) for the concentration of Xa bound to the platelet surface has terms corresponding to (G) fluid-phase Xa binding to and dissociating from P_{10} ; platelet-bound Xa transiently binding to platelet-bound factors V (H) and VIII (I) on the way to activating them; (J) platelet-bound Xa binding to platelet-bound Va to form the prothrombinase complex; and production of platelet-bound Xa by the tenase (VIIIa:IXa) (K) and tenase* (L)

subendothelium, and consequently platelet deposition progressively reduces TF:VIIa activity as the subendothelium becomes covered by platelets. With this addition to the model, large reductions in the concentration of factors VIII or IX lead to large drops in the production of thrombin, and the model also accurately captures the mild or severe reductions in thrombin production associated with moderate and severe thrombocytopenia, respectively. Recent experiments [3] provide strong support for our hypothesis that platelet deposits prevent transport to/from the subendothelial surface.

3 Model Extensions

The results presented in the current paper are based on extensions of the model we just reviewed. The most substantial change involves introduction of a more complete model of the protein C pathway. A second change relevant for some of the simulations presented below involves alternative schemes for the action of TFPI.

3.1 Protein C Activation Model

Protein C is activated to APC by a complex of thrombomodulin and thrombin on the surfaces of ECs [4], surfaces *geographically distinct* from the subendothelial surface on which the coagulation reactions occur. Because of the flow, it is unlikely that significant APC could reach the injured region from ECs upstream or downstream of the injury, because thrombin or APC, respectively, would have to move upstream against the flow for this to happen. Some thrombin produced in the reaction zone above the injury could diffuse laterally (perpendicular to the flow) to contact ECs adjacent to the injured region and there bind with TM (fig. 1b). APC activated by this complex could also diffuse laterally *into* the reaction zone above the injury and thereby be in a location to attack factors Va and VIIIa and perhaps affect subsequent thrombin production in the reaction zone. The amount of APC delivered to the thrombus by this mechanism depends on the extent of thrombin production in the reaction zone, the kinetics of thrombin binding to TM on ECs, and the kinetics of PC activation to APC by the thrombin-TM complex. It also depends on the number of thrombin and APC molecules that are able to diffuse between the reaction zone and the adjacent ECs before being carried downstream by the flow. To explore this, we add a second zone to our model; it consists of a thin volume over the adjacent endothelial surface, the same height \bar{h} and length L as the reaction zone over the injury, and a

width W_{ec} that is determined by the flow speed and protein diffusion coefficients as shown in the Appendix. In this ‘endothelial zone’, we track the concentration of thrombin, the binding of thrombin to TM, and the production of APC by the resulting complex. Fluid-phase molecules in the endothelial zone are susceptible to being carried downstream by the flow, and can diffuse laterally into the reaction zone. We introduce new variables for the endothelial zone concentrations of thrombin e_2^{ec} , APC $[APC]^{ec}$, the thrombin-TM complex $[TM : E_2]$, and the complex formed when PC binds to the thrombin-TM complex $[TM : E_2 : PC]$. The equations governing their dynamics are:

$$\frac{de_2^{ec}}{dt} = \underbrace{-k_{flow}^c e_2^{ec}}_A - \underbrace{k_2^{in} e_2^{ec}}_B + \underbrace{k_{diff}(e_2 - e_2^{ec})}_C - \underbrace{k_{tm}^{on} e_2^{ec}([TM] - [TM : E_2] - [TM : E_2 : PC]) + k_{tm}^{off}[TM : E_2]}_D \quad (3.1)$$

$$\frac{d[TM : E_2]}{dt} = \underbrace{k_{tm}^{on} e_2^{ec}([TM] - [TM : E_2] - [TM : E_2 : PC]) - k_{tm}^{off}[TM : E_2]}_D - \underbrace{k_{pc}^+ [TM : E_2][PC] + (k_{pc}^- + k_{pc}^{cat})[TM : E_2 : PC]}_E \quad (3.2)$$

$$\frac{d[TM : E_2 : PC]}{dt} = \underbrace{k_{pc}^+ [TM : E_2][PC] - (k_{pc}^- + k_{pc}^{cat})[TM : E_2 : PC]}_E \quad (3.3)$$

$$\frac{d[APC]^{ec}}{dt} = \underbrace{-k_{flow}^c [APC]^{ec}}_F + \underbrace{k_{diff}([APC] - [APC]^{ec})}_G + \underbrace{k_{pc}^{cat}[TM : E_2 : PC]}_H \quad (3.4)$$

Here, $[TM]$ is the total concentration of TM in the endothelial zone and $[PC]$ is the plasma concentration of protein C which we treat as constant (because a very small fraction of it is converted to APC). The terms in the equations describe (A) removal of thrombin by flow, (B) inactivation of thrombin by AT-III, (C) transport of thrombin by diffusion between the reaction zone and the endothelial zone, (D) thrombin binding to and dissociating from TM, (E) transient binding of the thrombin-TM complex to PC on the way to activating PC, (F) removal of APC by flow, (G) diffusion of APC between the zones, and (H) production of APC by the thrombin-TM complex. The kinetic parameters and plasma concentrations relevant

Table 1. APC pathway reaction parameters

Reaction	$M^{-1}s^{-1}$	s^{-1}	s^{-1}	
Thrombin binding with TM	$k_{tm}^{on} = 1.0(10)^8$	$k_{tm}^{on} = 0.05$		a
TM:Thrombin activation of PC	$k_{pc}^+ = 1.66(10)^6$	$k_{pc}^- = 1.0$	$k_{pc}^{cat} = 0.167$	b

a $K_d = 5.0(10)^{-10} M$ and $[PC] = 65 nM$ [9].
b $k_{pc}^{cat} = 0.167 s^{-1}$, $K_M = 0.7(10)^{-6} M$ [18], and $[TM] = 100$ to $2,500 nM$ [4].

for these equations are given in table 1. The extensions to the model also necessitate changes to the equations for the thrombin and APC concentrations in the reaction zone. The new versions of these equations are:

$$\frac{de_2}{dt} = \underbrace{-k_{diff}(e_2 - e_2^{ec})}_A - \underbrace{k_{flow}^c e_2}_B - \underbrace{k_2^{in} e_2}_C - \underbrace{k_2^{on} e_2 (p_2 - z_2^{mtot} - e_2^{mtot}) + k_2^{off} e_2^m}_D \quad (3.5)$$

$$+ \underbrace{(k_{12}^- + k_{12}^{cat}) [Z_5 : E_2] - k_{12}^+ z_5 e_2}_E + \underbrace{(k_{14}^- + k_{14}^{cat}) [Z_8 : E_2] - k_{14}^+ z_8 e_2}_F$$

$$+ \underbrace{(k_{18}^- + k_{18}^{cat}) [Z_7 : E_2] - k_{18}^+ z_7 e_2}_G + \underbrace{(k_3^- + k_3^{cat}) [Z_7^m : E_2] - k_3^+ z_7^m e_2}_H$$

$$\frac{d[APC]}{dt} = \underbrace{-k_{diff}([APC] - [APC]^{ec})}_I - \underbrace{k_{flow}^c [APC]}_J - \underbrace{k_{16}^+ [APC] e_5^m + (k_{16}^- + k_{16}^{cat}) [APC : E_5^m]}_K \quad (3.6)$$

$$- \underbrace{k_{17}^+ [APC] e_8^m + (k_{17}^- + k_{17}^{cat}) [APC : E_8^m]}_L$$

The new terms in these equations are for thrombin (A) and APC (I) diffusion between the reaction zone and endothelial zone. The remaining terms in the thrombin equation are for (B) removal of thrombin by the flow, (C) inactivation of thrombin by AT-III, (D) thrombin binding to and dissociation from the platelet binding sites (P_2) for thrombin and prothrombin, and transient thrombin binding to (E) factor V, (F) factor VIII, (G) factor VII, and (H) TF:VII, on the way to activating these cofactors or enzymes. The remaining terms in the APC equation describe (J) removal of APC by flow, and APC binding to and inactivating platelet-bound Va (K) and VIIIa (L). In some simulations, APC is assumed to attack fluid-phase factors Va and VIIIa, or both the platelet-bound and fluid-phase cofactors and then the terms (K) and (L) are modified accordingly.

3.2 Alternative Schemes for TFPI Action

The most widely-accepted scheme for the action of TPFI involves the sequential binding first of TPFI to factor Xa, and then of the TFPI:Xa complex to TF:VIIa [5]. We assumed that TFPI operates according to this ‘standard scheme’ in our original model [1] and for most of the simulations in the current paper. An alternative mode of action was suggested by Baugh et al. [6] and involves TFPI binding directly to Xa that is *already* bound to the TF:VIIa complex. We have formulated an alternative set of equations for TFPI and its complexes which embody this alternative scheme. For the standard scheme we assumed that when X bound to TF:VIIa is activated to Xa, the Xa molecule immediately dissociates. To implement the alternative scheme, we allow for a finite rate of Xa dissociation from TF:VIIa so that Xa can remain bound to TF:VIIa after its activation. The concentration of the complex of Xa bound to TF:VIIa appears as a new variable $[E_{10} : E_7^m]$ in the alternative model and a new differential equation is added to describe the dynamics of this concentration. A number of other equations are modified from their form in the standard model. Eq (3.7) is the new equation, and Eqs (3.8) and (3.9) are two of the modified equations.

$$\frac{d[E_{10} : E_7^m]}{dt} = \underbrace{k_8^{cat} [Z_{10} : E_7^m]}_A - \underbrace{k_8^{*-} [E_{10} : E_7^m] + k_8^{*+} e_7^m e_{10}}_B - \underbrace{k_8^+ [TFPI] [E_{10} : E_7^m] + k_8^- [TFPI : E_{10} : E_7^m]}_C - \underbrace{[E_{10} : E_7^m] \frac{p'}{1-p}}_D \quad (3.7)$$

$$\frac{d[TFPI]}{dt} = \underbrace{-k_{10}^+ [TFPI] e_{10} + k_{10}^- [TFPI : E_{10}]}_E + \underbrace{k_{flow}^c ([TFPI]^{out} - [TFPI])}_F - \underbrace{k_8^+ [TFPI] [E_{10} : E_7^m] + k_8^- [TFPI : E_{10} : E_7^m]}_C \quad (3.8)$$

$$\begin{aligned}
\frac{d[TFPI : E_{10} : E_7^m]}{dt} = & \\
& \underbrace{-k_{11}^- [TFPI : E_{10} : E_7^m] + k_{11}^+ [TFPI : E_{10}] e_7^m}_{G} \\
& \underbrace{+k_8^+ [TFPI] [E_{10} : E_7^m] - k_8^- [TFPI : E_{10} : E_7^m]}_C \\
& \underbrace{-[TFPI : E_{10} : E_7^m] \frac{p'}{1-p}}_H
\end{aligned} \tag{3.9}$$

The terms in Eq (3.7) describe (A) activation of X to Xa while bound to TF:VIIa, (B) Xa binding to and dissociating from TF:VIIa, (C) TFPI binding to and dissociating from the TF:VIIa:Xa complex, and (D) the effective loss of TF:VIIa:Xa as the subendothelium becomes covered by platelets. (This is described further below.) Eq (3.8) contains additional terms which reflect (E) plasma-phase binding and unbinding of TFPI with Xa, and (F) transport of TFPI with the moving plasma. The terms (G and C) in Eq (3.9) describe the two ways of forming the TF:VIIa:TFPI:Xa complex, and term (H) describes the loss of accessible complex as platelets cover the subendothelium. Two other equations are modified in the alternative model; in Eq (2.1) for e_{10} , the concentration of fluid-phase Xa, the term (A) $k_8^{\text{cat}} [Z_{10} : E_7^m]$ is removed and the terms (B) from Eq (3.7), $k_8^{*-} [E_{10} : E_7^m] - k_8^{*+} e_7^m e_{10}$, are added. These changes reflect the new assumption that the rate of dissociation of Xa from TF:VIIa is finite. The same changes are made in the equation (not shown) for the TF:VIIa concentration, e_7^m . A term like (D) appears in the kinetic equation for each species that involves TF. The variable p denotes the fraction of subendothelial area covered by platelets; p' is the rate of change of p , and the expression $-p'/(1-p) = (1-p)'/(1-p)$ is the fractional rate of change of uncovered subendothelial area. So term (D) in Eq (3.7) says that the concentration of TF:VIIa:Xa decreases at a fractional rate equal to the fractional rate of decrease of uncovered subendothelial area.

4 Results

Since the model has been modified significantly from that in [1], we investigated whether the new version retains the threshold-dependence of thrombin production on the density of TF exposed. For each of several values of the flow shear rate ($\gamma = 2V/R$), we computed³ the con-

³ The model equations were solved numerically using a standard Fortran package LSODE for solving ordinary differential equations [7].

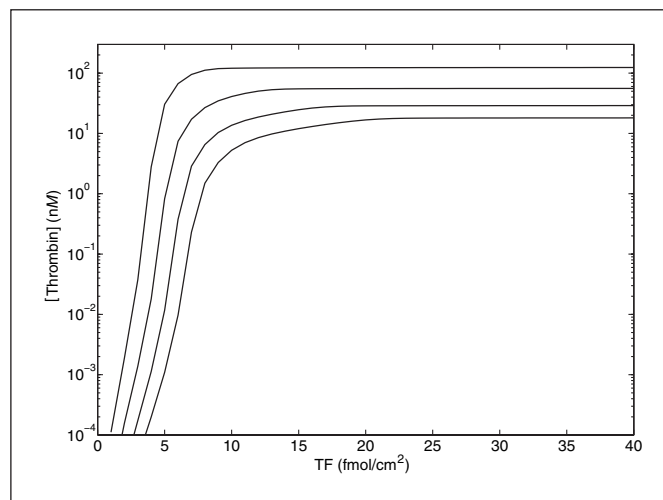


Fig. 3. Thrombin concentration after 10 min for different levels of TF exposure and different shear rates. Curves top to bottom are for shear rates 10, 100, 500, 1,500 s^{-1} . [TM] = 500 nM.

centration of thrombin 10 min after TF exposure as a function of the density of TF exposed. The results of these calculations are presented in figure 3 and show that the new model does indeed still show sharp thresholds in response to TF variations for each of the shear rates examined. In this section, we describe results of simulation experiments to investigate the determinants of the threshold behavior. We then turn to examining the roles of the chemical inhibitors APC and TFPI. The common thread linking the three sets of experiments is the substantial influence of flow.

4.1 Early Determinants of High Thrombin Production

In order to understand what distinguishes the below-threshold response from the above-threshold one, and thus leads to such dramatically different levels of thrombin production, we looked at early events in the model response for three densities of exposed TF (3, 5, and 15 $fmol/cm^2$) that span the transition from below- to above-threshold densities at a shear rate of $\gamma = 100 s^{-1}$. We find that, in essence, the difference in behavior is due to the outcome of a race on the subendothelial and platelet surfaces. Recall that an important assumption of our model is that each platelet adherent to the subendothelium blocks access to the surface reactants (including TF:VIIa) on a portion of the subendothelium, and so the activity of TF:VIIa is progressively reduced as the subendothelium is covered by platelets. The speed at which the subendothelium becomes covered is determined by the

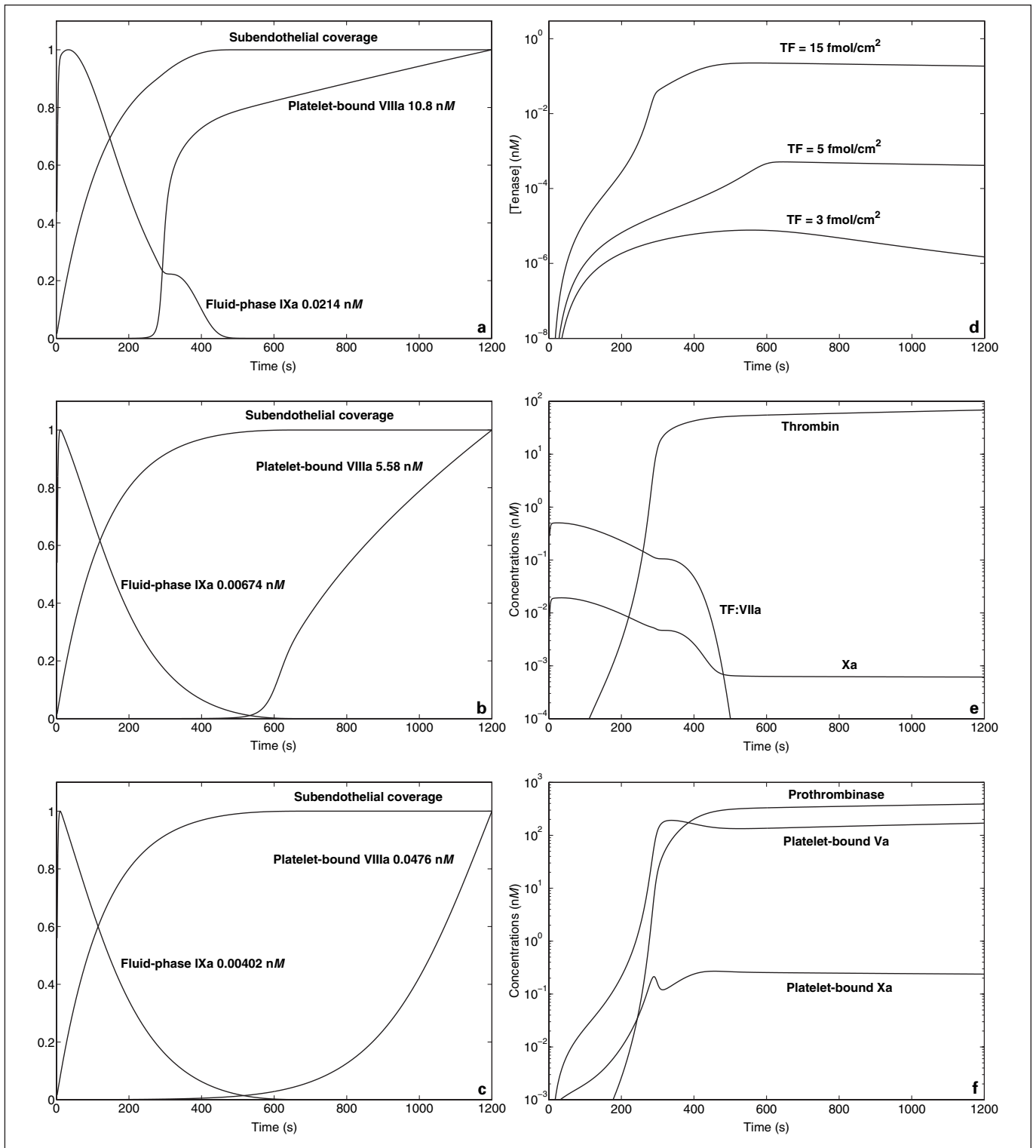


Fig. 4. a–c Scaled values of the fluid-phase IXa and platelet-bound VIIIa concentrations and the fraction of the subendothelium covered by platelets for TF density **a** 15, **b** 5, and **c** 3 fmol/cm². The concentrations are scaled by their maximum values (indicated) in the experiment. **d** Time course of tenase concentration for each of

the three levels of exposed TF. For TF density 15 fmol/cm², time course of **e** TF:VIIa, fluid-phase Xa, and thrombin concentrations and **f** platelet-bound Va and Xa, and prothrombinase concentrations. (Shear rate 100 s⁻¹, [TM] = 500 nM.)

rate of transport of platelets into the reaction zone and the rate of attachment of these platelets to the subendothelium. As described in [1], the platelet transport rate is determined by the physical processes of flow and diffusion, and we set the platelet attachment rate so that the 10-by-10- μm piece of subendothelium exposed in our simulations is completely covered in about 5 min, consistent with estimates derived from Turitto et al. [8]. The time it takes for the subendothelium to be covered by platelets is only weakly affected by coagulation events (see below), and so the length of time during which TF:VIIa complexes on the subendothelium remain active is largely independent of the density of TF that is assumed to be exposed (see fig. 4a–c).

For the three densities of exposed TF considered, the peak densities of TF:VII and TF:VIIa increased in proportion to the TF density, and consequently the rate of production of enzymes IXa and Xa by TF:VIIa also increased proportionately. Within the model, the possible fates of a IXa molecule after its activation by TF:VIIa and release into the fluid include (i) being washed away by the flow, (ii) being inactivated by AT-III, and (iii) reversibly attaching to the surface of an activated platelet by binding to the platelet binding sites (P_1 and P_2^*) for IXa. In the last case, the binding is made firmer if there is VIIIa bound to the platelet surface and the bound VIIIa and IXa come together to form the tenase complex. It is only when sufficient platelet-bound VIIIa is present that IXa is protected against removal by flow or inactivation by AT-III. If little or no VIIIa is present, then continued production of IXa is required for significant concentrations of IXa to be maintained because the rate of removal of IXa nearly balances its rate of activation by TF:VIIa (see below). Because of platelet deposition, activation of IXa by TF:VIIa eventually stops, and so an important consideration is how rapidly VIIIa is activated during the time-window in which IXa is being produced by TF:VIIa. The two mechanisms in the model for activation of factor VIII to VIIIa involve Xa or thrombin as the enzyme, but because the thrombin concentration is extremely low early in the clotting response, only the Xa-mediated activation is relevant then.

For a TF density of 15 fmol/cm², which is well-above threshold, Xa and IXa are produced by TF:VIIa at a relatively rapid rate, and their concentrations within the reaction zone increase rapidly and persist at relatively high levels for several minutes (see fig. 4a, e). During this period, Xa activates platelet-bound VIII to VIIIa and IXa binds to platelets and becomes incorporated into tenase complexes. The overlap of the time intervals during which

the IXa concentration in the fluid and the platelet-bound VIIIa concentration are high, is critical to the formation of substantial amounts of the tenase complex on the platelet surfaces. As shown in figure 4a, this overlap is substantial for the case of TF density 15 fmol/cm². By contrast, at low TF densities, the concentration of Xa remains low. Little VIIIa is produced, so only a small amount of VIIIa binds to platelets during the period in which IXa is being produced by TF:VIIa. Figure 4c shows that, for a TF density of 3 fmol/cm², there is little overlap of the time intervals during which both IXa and platelet-bound VIIIa are present and, furthermore, the concentrations of both of these factors are low during the overlap period, so little tenase is formed. Consequently, amplification of the initial TF signal is greatly muted and little thrombin is produced. For a TF density of 15 fmol/cm², formation of substantial amounts of tenase occurs. The Xa activated by the tenase complex is already on a platelet's surface and so is sheltered from the effects of flow and inactivation by AT-III, and is ready to bind with platelet-bound Va to form prothrombinase. For a TF density of 5 fmol/cm², the situation is intermediate between those already shown; there is some overlap in the presence of IXa and platelet-bound VIIIa (see fig. 4b), and so there is some tenase formation and thrombin production. Relative to the 15 fmol/cm² case, tenase, prothrombinase, and thrombin production are delayed and the levels reached are substantially lower.

TF:VIIa-activated IXa and Xa face multiple barriers that may prevent them from reaching an activated platelet's surface. In our simulations, the most significant of these is removal by flow. Figure 5 shows the rate of production of IXa by TF:VIIa, its rate of removal by flow, and its rate of inactivation by AT-III at a shear rate of 100 s⁻¹. (The rates for Xa are similar and not shown.) The effect of AT-III is apparent, but it is substantially smaller than the physical effect of the flow in removing the enzymes. At shear rate 100 s⁻¹, the rates of removal of Xa and IXa by flow are about 80 times their respective rates of inactivation by AT-III. At higher shear rates the ratio of these rates is larger, and even at the very low shear rate of 10 s⁻¹, the ratio is about 15. Figure 5 also shows that the rate of removal of IXa tracks and almost equals its rate of production, so there is little opportunity for these molecules to accumulate in flow situations. The same observations pertain for Xa (not shown).

One of the positive feedback loops in the coagulation network involves Xa activating TF:VII to TF:VIIa. If this loop had a significant role under the setting of our simulations, we would expect to see a more-than-propor-

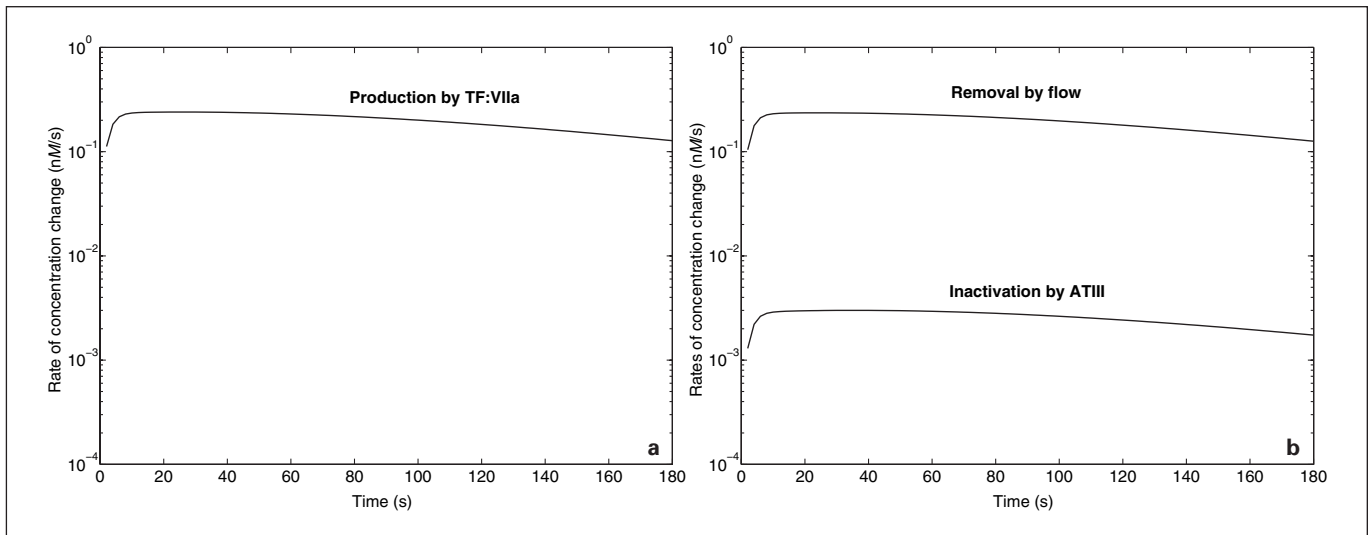


Fig. 5. a Rate of production of IXa by TF:VIIa. **b** Rate of removal of fluid-phase IXa by flow and rate of inactivation of fluid-phase IXa by AT-III. Note that the rate of removal by flow is much greater than the rate of inactivation by AT-III, and that the total rate of removal by flow and AT-III is nearly equal to the rate of production by TF:VIIa. (Shear rate 100 s^{-1} , $[\text{TM}] = 500 \text{ nM}$.)

tional increase in the rate of IXa and Xa production by TF:VIIa as the TF density is increased. As noted above, the rates of IXa and Xa production for the first several minutes rose in proportion to the level of exposed TF, so this feedback loop seems not to be significant here. A second feedback involves thrombin activation of TF:VII to TF:VIIa, and in Figure 4e we see that this sometimes affects the TF:VIIa concentration. At above-threshold densities of TF and at low shear rates, there is an upward ‘bump’ in the TF:VIIa concentration after about 5 min, and a corresponding bump in the fluid-phase Xa concentration. That the TF:VIIa bump is due to thrombin was confirmed by simulations (not shown) in which prothrombinase activity was turned-off and the bump disappeared. The relative size of the bump decreases with increasing shear rate and is not visible in graphs for shear rates 500 s^{-1} or above; this is consistent with the decrease in the thrombin concentration achieved as shear rate is increased. When present at all, the bump is temporary because subendothelial coverage by platelets continues to increase. We also note that the drop in the concentration of platelet-bound Xa starting at 270 s (see fig. 4f) and that of platelet-bound Va a little later are due to their combination into the prothrombinase complex. The Va concentration drop occurs later because it is offset by the release and subsequent activation of V from activated platelets.

While the rate of platelet deposition on the subendothelium is essentially independent of coagulation events for the early portion (the first 3 min) of our simulations, the level of thrombin production does have some effect after this period. This can be seen in figure 4a–c in which subendothelial coverage is complete at about 420 s for a TF density of 15 fmol/cm^2 , while the last few percent of uncovered subendothelium do not disappear until almost 600 s at low TF densities. The reason for this difference is somewhat subtle as the model assumes that for platelets within the reaction zone the rate of adhesion to the exposed subendothelium is the same for unactivated platelets and for platelets already activated by thrombin. The difference arises because platelets activated in any way are assumed to become part of a stationary aggregate and so are no longer a factor in determining the delivery of additional unactivated platelets to the reaction zone by flow and diffusion. The rate of such transport depends on the concentration difference for unactivated platelets between the bulk fluid and the reaction zone; this is increased when the rate of activation of platelets is increased. The slower coverage of the subendothelium at low TF densities actually gives the system a longer window in which to achieve overlap between significant IXa and platelet-bound VIIIa concentrations than is present in the high TF case. Even so, the overlap is inadequate to lead to a substantial response.

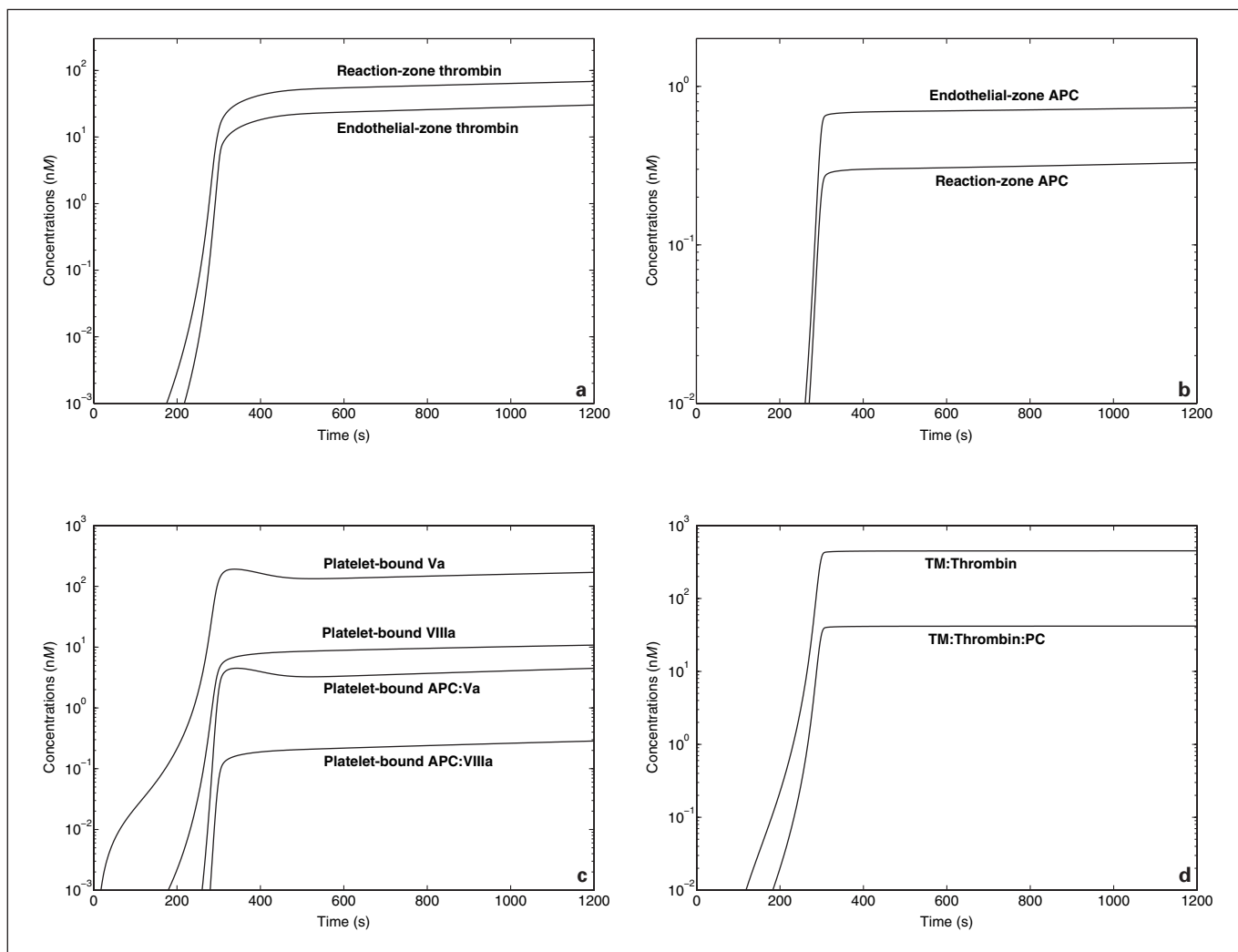


Fig. 6. **a** Concentration of thrombin in the reaction and endothelial zones. **b** Concentrations of APC in the reaction and endothelial zones. **c** Concentrations of platelet-bound VIIIa, platelet-bound VIIIa bound to APC, platelet-bound Va, and platelet-bound Va bound to APC. **d** Concentrations of the TM complexes in endothelial zone. (Shear rate 100 s^{-1} , $[\text{TM}] = 500 \text{ nM}$.)

4.2 APC-Mediated Inhibition under Flow

In this section, we consider the effect of APC on the concentrations of thrombin attained in the model system. Two modes of APC delivery to the reaction zone are considered. The first is embodied in the model discussed in Section (3.1); it involves APC production on endothelial cells adjacent to the reaction zone, and its transport by diffusion into the reaction zone. The other assumes that the plasma APC concentration is determined systemically (e.g., as a result of thrombin produced at locations throughout the circulation) and that APC is delivered to the reaction zone by flow and diffusion like other plasma-

borne proteins. We also consider various targets of APC action: platelet-bound Va and VIIIa, fluid-phase Va and VIIIa, or both.

For APC production on adjacent ECs according to Eqs (3.1–3.4), important parameters are the flow speed and the concentration of thrombomodulin. The faster the flow, the less effective is transport of thrombin from the reaction zone to the endothelial zone and of APC in the reverse direction (see Appendix). We focus on a slow flow (shear rate 100 s^{-1}) characteristic of the venous circulation. Esmon [4] suggests that the thrombomodulin concentration in the microcirculation is between 100 and

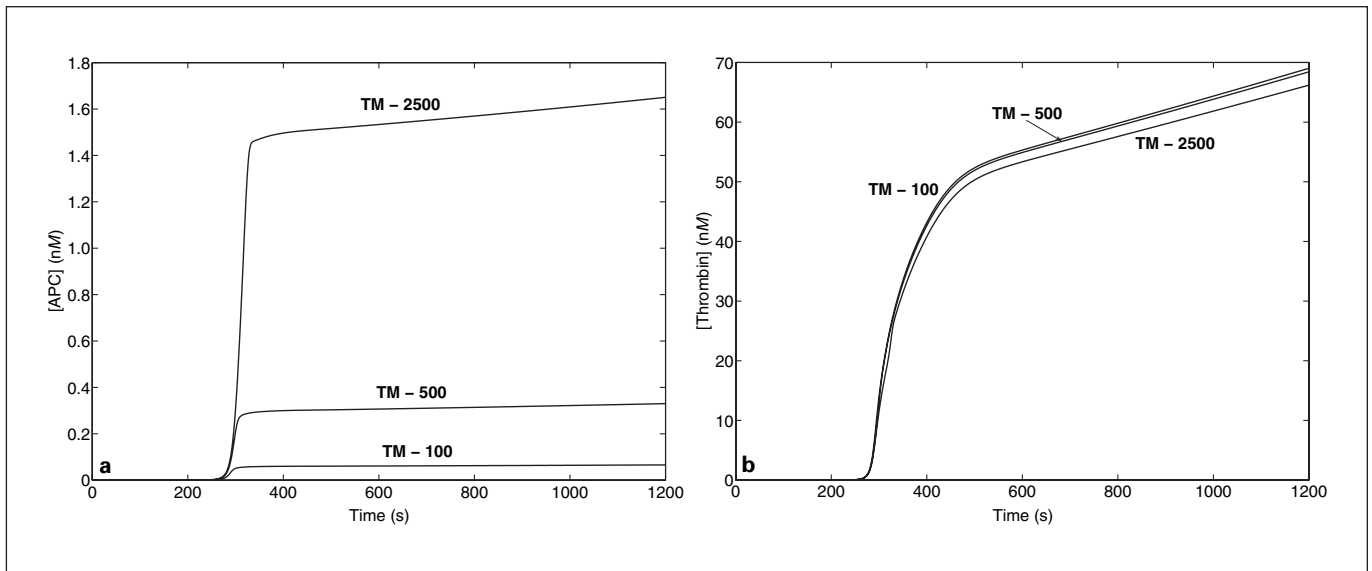


Fig. 7. **a** Concentrations of APC in the reaction zone for thrombomodulin concentrations 100, 500, and 2,500 nM. **b** Concentrations of thrombin in the reaction zone for these TM concentrations. (Shear rate 100 s^{-1} .)

500 nM. We considered three different thrombomodulin levels: 100, 500 and 2,500 nM. Figure 6 shows the time-course of various concentrations for a TM concentration of 500 nM and under the assumption that APC inactivates only platelet-bound Va and VIIIa. We see a significant APC concentration only after about 250 s; this period corresponds to the lag before substantial thrombin production. The thrombin concentration in the reaction zone reaches about 68 nM, while that in the endothelial zone, limited by the transport of thrombin from the reaction zone (through the coefficient k_{diff}), reaches only about 30 nM. As substantial amounts of thrombin are produced, most of the TM quickly becomes bound to thrombin (either thrombin alone or with PC), the concentrations of these complexes remain roughly constant after this (see fig. 6d), and the TM:thrombin complex produces APC sufficient to bring its concentration to about 0.73 nM in the endothelial zone. Transport limits the transfer between zones, and the APC concentration in the reaction zone reaches an approximate plateau at about 0.33 nM (see fig. 6b). As shown in figure 6c, there are significant amounts of APC bound to platelet-bound Va and VIIIa, on its way to proteolytically inactivating them, but the APC concentrations are not enough for this to prevent the continued gradual increase in the concentrations of platelet-bound Va and VIIIa. Similar simulation experiments were done with TM concentrations of 100 and 2,500 nM. The plateau concentrations of APC in the re-

action zone increased approximately in proportion to the change in TM concentration (see fig. 7a), as essentially all of the TM was bound to thrombin in each experiment. The effect on the concentration of thrombin in the reaction zone was small, as shown in figure 7b; increasing the TM concentration by 25-fold reduced the resultant thrombin concentration within the reaction zone by only about 4%. The effect of APC on thrombin production was only slightly different in simulations in which fluid-phase Va and VIIIa were the only targets of APC, in which platelet-bound Va and VIIIa were the only targets (as above), or in which both the fluid-phase and platelet-bound cofactors were targets. In these three cases, the concentrations of thrombin present after 20 min were 69.2, 68.4, and 66.2 nM, respectively.

In figure 8 we show how the effectiveness of the APC-pathway is influenced by the flow speed. From experiments with shear rates of 100, 500, and $1,500 \text{ s}^{-1}$, we see that as the shear rate is increased: (i) the flux of thrombin from the reaction zone to the endothelial zone decreases (fig. 8a); (ii) the concentration of APC produced by the TM:thrombin complex in the endothelial zone decreases (fig. 8b); (iii) the flux of APC from the endothelial zone to the reaction zone decreases (fig. 8c); and iv) the rate of inactivation of platelet-bound VIIIa and Va by APC in the reaction zone decreases (fig. 8e). This last occurs despite a substantial increase in the concentrations of the target molecules, platelet-bound VIIIa and Va, with in-

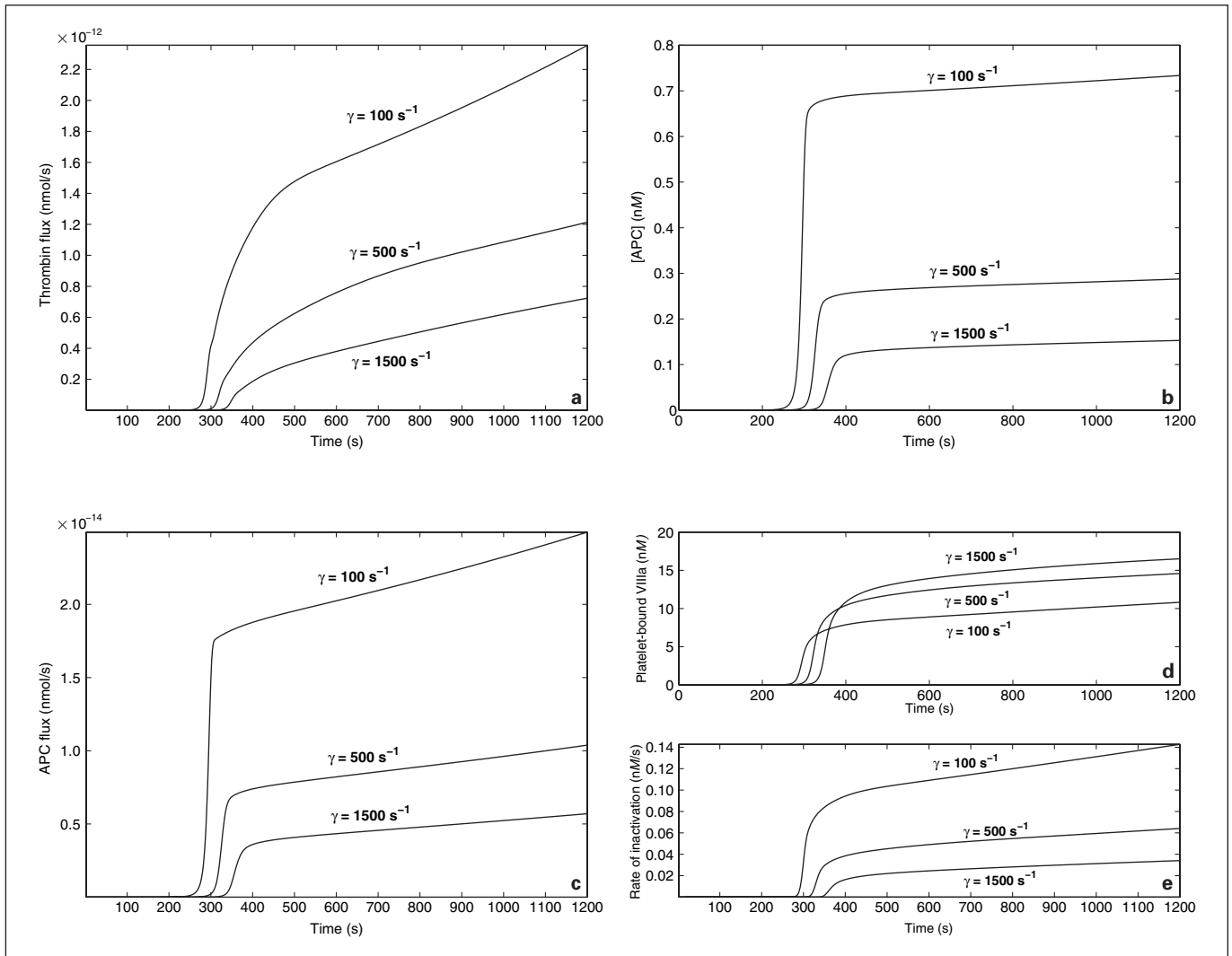


Fig. 8. For each of the three shear rates 100, 500, and 1500 s^{-1} . **a** Flux of thrombin from reaction zone to endothelial zone. **b** Concentration of APC produced in endothelial zone. **c** Flux of APC from endothelial zone to reaction zone. **d** Concentrations of platelet-bound VIIIa. **e** Rate of inactivation of platelet-bound VIIIa by APC. ([TM] = 500 nM.)

creasing shear rate (see fig. 8d) which itself is a result of the increased rate of delivery of zymogens to the reaction zone at high shear rates. The overall effectiveness of APC in limiting thrombin production decreases substantially as the flow speed goes up.

We also looked at how the model system behaves when APC is delivered to the reaction zone at a *prescribed* concentration, rather than being produced in response to local thrombin production. Figure 9 shows the thrombin concentration in the reaction zone at time 10 min for experiments differing only in the prescribed APC concentration. We clearly see that at plausible levels of APC, such as the

40-pM level at which APC is reported to circulate [9], thrombin production is virtually unaffected. As the prescribed APC concentration is increased to levels approaching 10 nM or more, i.e., levels that are a substantial fraction of the total PC concentration in the plasma, thrombin production drops dramatically, so that at a concentration of half the normal PC concentration (65 nM), the maximal concentration of thrombin is sub-picomolar.

4.3 TFPI-Mediated Inhibition under Flow

Results from [1] show that for a scheme of TFPI-mediated inhibition of TF:VIIa in which there is sequential

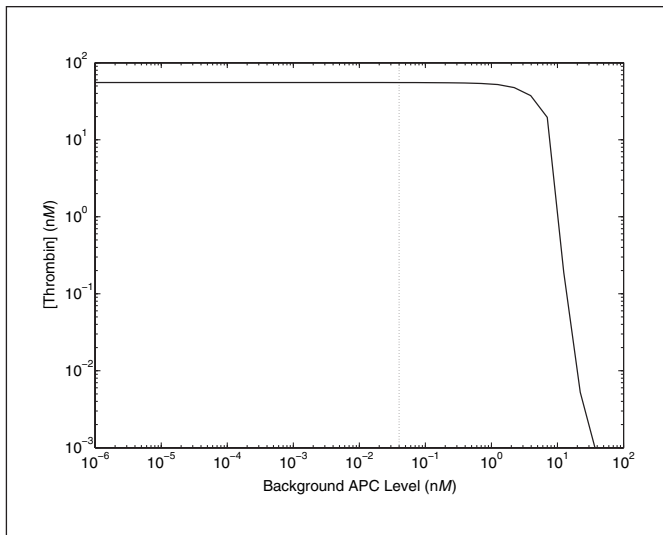


Fig. 9. Concentration of thrombin after 10 min for TF density 15 fmol/cm^2 and for varying levels of the prescribed plasma APC concentration. The dotted line at 40 pM indicates the measured plasma APC concentration. (Shear rate 100 s^{-1} , $[\text{TM}] = 500 \text{ nM}$.)

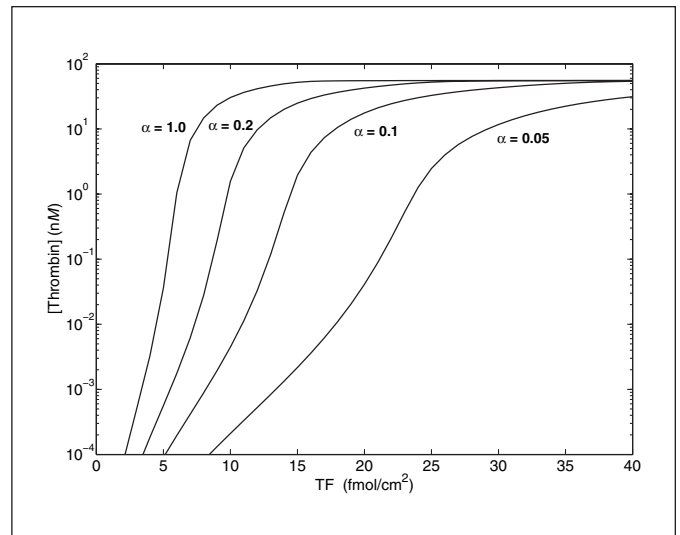


Fig. 10. Thrombin concentration at 10 min for various densities of TF and for several values of the Xa-TF:VIIa binding/unbinding rates scale factor α . (Shear rate 100 s^{-1} , $[\text{TM}] = 500 \text{ nM}$.)

binding, first of TFPI to Xa, and then of TFPI:Xa to TF:VIIa, TFPI has virtually no effect on the model's behavior. This is true also for the modified model presented here in which the APC pathway is modeled as described in Section 3.2. For example, curves like those in figure 3, but generated in simulations in which the TFPI concentration was set to zero, were visually indistinguishable from those in figure 3. Below we present results for an alternative scheme in which TFPI binds to Xa that is already bound to TF:VIIa, as proposed in [6], and which we model using the equations discussed in Section 3.2.

TF:VIIa is activated by Xa and an important issue for the alternative scheme is how rapidly Xa dissociates from the TF:VIIa complex. Mann [10] give K_M and k_{cat} values for TF:VIIa's activation of X to Xa, and in our earlier paper, we used these to estimate the rates of binding and unbinding of X with TF:VIIa. Here we assume that the ratio of the unbinding rate to the binding rate for X also pertains to Xa i.e., we assume that the dissociation constant is the same) and we perform simulation experiments in which both rates are scaled by a common factor α which therefore changes the speeds at which Xa binds and unbinds but does not change the dissociation constant K_d . For small values of the scale factor α , the unbinding of Xa from the TF:VIIa complex is relatively slow, and so TFPI has a relatively long period during which to bind to the bound Xa. However, during the period that Xa is

bound to a TF:VIIa complex, it is not necessary for TFPI to also bind in order that the activity of that complex be inhibited; the bound Xa already accomplishes this.

Figure 10 shows that as the scaling parameter is changed the threshold level of TF exposure changes significantly. However, this behavior is *not* due to TFPI, as parallel experiments done with *no* TFPI present produce curves virtually indistinguishable from those shown. The results shown in figure 10 are for shear rate 100 s^{-1} , but the absence of an effect of TFPI holds true for all shear rates considered from 10 to $1,500 \text{ s}^{-1}$. The differences we see are instead caused by the different degrees of inhibition of TF:VIIa provided by bound Xa at different rates of Xa unbinding.

We illustrate the behavior of the alternative model for two values of the scaling parameter α and for a TF density of 15 fmol s^{-1} . Figure 11a–b shows results for the $\alpha = 1.0$ case, in which binding and unbinding of Xa from TF:VIIa occur at the same rates previously assumed for X's binding reactions with TF:VIIa. The results for this case are very similar to those from simulations in which Xa is assumed to dissociate instantaneously from TF:VIIa (see fig. 4a, e, f). The maximum concentrations of fluid-phase IXa and Xa and of platelet-bound VIIIa are a little less than in the instantaneous dissociation case, but we see that there is again substantial overlap in the periods during which significant fluid-phase IXa and

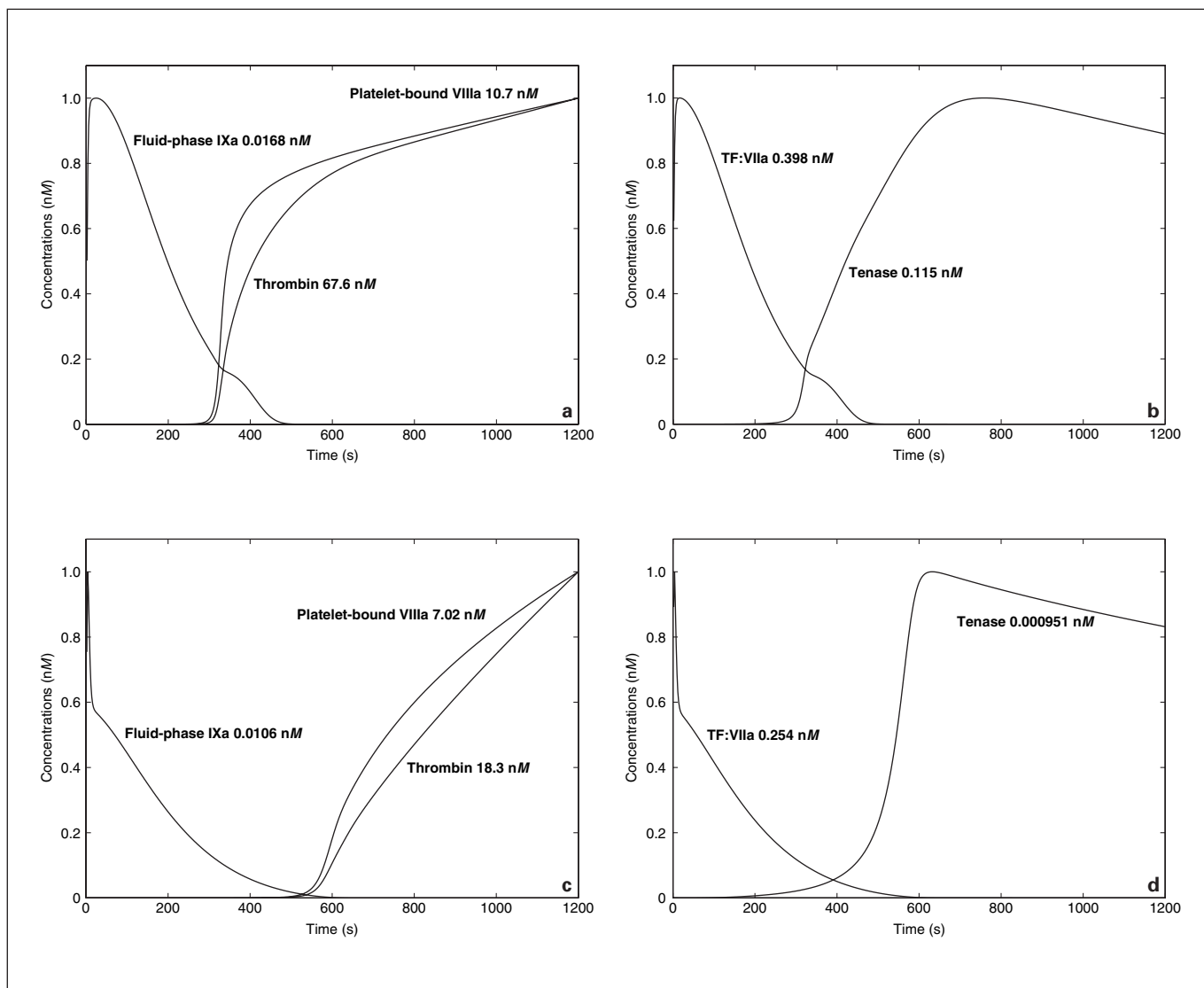


Fig. 11. Left: Time course of platelet-bound VIIIa, fluid-phase IXa, and thrombin concentrations. Right: Time course of TF:VIIa and tenase concentrations. **a, b** Xa-TF:VIIa binding/unbinding scale factor $\alpha = 1.0$. **c, d** Xa-TF:VIIa binding/unbinding scale factor $\alpha = 0.1$. (Shear rate 100 s^{-1} , $[\text{TM}] = 500 \text{ nM}$.)

platelet-bound VIIIa coexist and this leads to tenase formation and eventually to thrombin concentrations only a little different from those in figure 4e. The results with $\alpha = 0.1$ are shown in figure 11c–d, and we see that there is much less thrombin production in this case. We also see that following the usual initial sharp rise in the concentrations of TF:VIIa and fluid-phase IXa, both of these concentrations drop very sharply concomitant with a steep rise in the concentration of TF:VIIa:Xa as Xa is activated but remains bound to TF:VIIa. The concentration of unbound and therefore active TF:VIIa after this

sharp drop is approximately equal to the maximal concentration of TF:VIIa available with an exposed TF density of 5 fmol/cm^2 for the standard model of TPF1 action, and the subsequent story here is just about the same as there (see fig. 4b): Since IXa and Xa are produced at a slower rate, there is a substantial delay in the intervals of overlap of fluid-phase IXa and platelet-bound VIIIa, and the quantities of each of these are small when they do overlap. Hence, tenase production is delayed and weak, and thrombin production is limited because of this.

5 Discussion

Using mathematical models, we have looked at the interactions among coagulation biochemistry, platelet deposition and activation, and flow-mediated transport of platelets and coagulation proteins in the response to vascular injury.

The models take into account plasma-phase and surface-bound enzymes and zymogens, coagulation inhibitors, and activated and unactivated platelets. They include both plasma-phase and membrane-phase reactions, and account for chemical and cellular transport by flow and diffusion. The models extend the model we published earlier [1] by incorporating more accurately the chemistry of APC activation as well as the necessity of transport of thrombin from the injured region where it is produced to the ECs where APC is activated, and of APC in the reverse direction. This transport is strongly influenced by the blood's velocity and we have elucidated this dependence and studied its consequences. The model also treats the inhibition of TF:VIIa by TFPI. In the standard version of the model, TFPI acts through sequential binding, first of TFPI to Xa, followed by that of TFPI:Xa to TF:VIIa. With this pathway, we see almost no effect of TFPI in determining the conditions under which substantial amounts of thrombin are produced or on the amount of thrombin produced when those conditions are met. We introduced a variant of our model in which TFPI acts by binding to a Xa molecule that is already bound to TF:VIIa, a pathway proposed by Baugh et al. [6], and examined the effectiveness of TFPI inhibition via this mechanism.

The new models, like that presented in [1], show a threshold response to TF exposure (with 1% of circulating plasma VII assumed to be in the active VIIa form). For low TF densities (fig. 3), little thrombin is produced. For high TF densities, there is a lag period of several minutes during which the thrombin concentration slowly increases through the picomolar range, followed by a sharp increase over another minute or so to a tens of nanomolar level (fig. 4e). Both the threshold response and the two stage temporal behavior, an initiation phase followed by an explosive phase when above threshold, have been reported in experimental studies [e.g., 2] and in other models [11].

There is little difference in the final thrombin concentration achieved for our model for different values of the exposed TF density that are all above the threshold level. Threshold behavior in a dynamical system is the result of competition between one or more nonlinear amplifica-

tion processes and one or more inhibitory processes. The system has little net response if the initiating stimulus is insufficient to overcome the inhibition; on the other hand, if the stimulus is strong enough to push the system over the inhibitory barrier, the nonlinear amplification kicks in and there is a very potent response. Van't Veer [2] shows evidence that the inhibitory barrier in their experimental system is due to the action of TFPI and AT-III. Their experiments involved a reconstituted plasma system with TF relipidated in phospholipid vesicles, the concentration of TF held constant and in excess, and the concentration of exogenous VIIa varied. No flow or platelets were involved and so zymogens were depleted over time and enzyme concentrations grew. The situations to which our models pertain are very different in that they involve flow and platelets. As noted in Section 4.3, TFPI plays an insignificant role in determining the necessary level of TF exposure to elicit explosive thrombin production or the final concentration of thrombin produced. AT-III has some inhibitory influence, but the dominant barrier that the system has to overcome for explosive thrombin production to occur is physical. Factors IXa and VIIIa have to be produced sufficiently rapidly, during the period before platelets cover the subendothelium, so that a significant tenase presence is established on platelet surfaces even though most of the IXa and Xa (Xa activates VIIIa) produced by subendothelial TF:VIIa is carried away by flow. Whether the tenase complex gets a sufficient foothold is therefore influenced predominantly by the level of TF exposure and the speed of the blood flow.

We also looked at the role that APC plays in controlling thrombin production. APC is produced on ECs as a consequence of the binding of thrombin to thrombomodulin on these cells. Similarly to the case of IXa and Xa which are produced on one surface, the subendothelium, and exert their effect on another surface, that of activated platelets, thrombin produced on the surface of activated platelets near the injury has to make its way to a distinct location, the surface of ECs, and for APC to possibly affect thrombin production, it has to make the reverse trip. The ability of these molecules to make these trips depends on the relative locations of the injured region and the ECs with respect to the flow direction, as well as on the speed of the flow. Molecular diffusion is the only means for thrombin and APC molecules to move in directions other than downstream with the flow. The effectiveness of diffusive transport decreases as the flow speed increases, simply because the molecules have less time to diffuse

before they are carried downstream. We built a model of APC production on ECs adjacent to the injury and with transport between the injury and the ECs determined by the molecular diffusivity and the flow speed. For a range of flow speeds and assumed levels of thrombomodulin on ECs, we explored how much APC was produced, how much of this APC reached the injured region, and how significant a role it played in inactivating coagulation cofactors Va and VIIIa. At a shear rate of 100 s^{-1} , typical of the venous circulation, a 25-fold increase in TM concentration caused only a small decrease in thrombin production (fig. 7). APC did inactivate VIIIa and Va, but at a rate insufficient to prevent continued increases in the VIIa and Va concentrations during the course of a simulation experiment. At higher shear rates, the effectiveness of APC was even weaker because, on the one hand, the rate at which it inactivated the cofactors was lower because transport limitations led to lower APC concentrations near the injury, and on the other hand, the rates at which the active cofactors were produced increased as the shear rate increased. Since some studies [12] suggest that APC is not effective against platelet-bound VIIIa or Va, we also simulated the model's behavior if fluid-phase VIIa and Va were the target of APC, or if both the fluid-phase and platelet-bound cofactors were susceptible to inactivation by APC. In all cases, APC was ineffective. Overall, APC produced on adjacent ECs played a minor role as an inhibitor of coagulation in the vicinity of the vascular injury.

TFPI is regarded as a significant inhibitor of coagulation, but we saw no evidence to support this contention in our simulations. For mechanisms of TFPI action involving either (i) sequential binding of TFPI and Xa and then TFPI:Xa and TF:VIIa, or (ii) binding of TFPI to Xa already bound to TF:VIIa, we saw virtually no difference in thrombin production between simulations in which the TFPI concentration was set to its plasma level (2.5 nM) and simulations from which TFPI was absent.

The models we have been exploring involve a comprehensive description of the biochemistry of the tissue factor pathway of coagulation. They use kinetic parameters and protein concentrations derived from the literature and believed to be characteristic of normal blood. Yet, in contrast to prevailing views of the importance of the chemicals TFPI, APC, and AT-III in regulating coagulation, we saw virtually no (for TFPI) or little (for APC and AT-III) influence of these molecules on thrombin production. Instead, what we saw to be the dominant 'inhibitors' of thrombin production at a small injury were *physical* factors: transport by flow and diffusion, platelet deposi-

tion, and the occurrence of important reactions on geographically distinct surfaces. We certainly do not contend that TFPI, APC and AT-III are irrelevant. TFPI on endothelial cells, APC produced on those cells, and AT-III in plasma may be essential in limiting the spread of coagulation beyond the injury site by scavenging and inactivating active coagulation factors that are carried downstream by the flow.

What we do argue is the importance of conducting experiments that include the physical factors discussed above. Important steps in that direction have been taken, for example, by Hoffman, Monroe, and co-workers in their studies of coagulation in the presence of platelets and other TF-bearing cells [13, 14], and by Nemerson and co-workers in looking at the effect of flow and transport on small portions of the coagulation system [3, 15, 16]. We hope that such efforts are extended to include more of the physical factors that are likely to play important roles in vivo.

6 Appendix: Transport between Reaction and Endothelial Zones

In [1], we determined the height \bar{h} of the reaction zone by estimating the height of the region from which a molecule above the injury could diffuse to the vessel wall before being carried past the injured region by flow. We found $\bar{h} = 3/4 (RLD/V)^{1/3}$, where V is the blood velocity at the vessel's center-line, R is the vessel's radius, L is the length of the injury, and D is the molecule's diffusion coefficient. Now we want to estimate how far a molecule, such as thrombin, starting in the reaction zone, can diffuse laterally before being carried past the injury by the flow. The average fluid velocity in the reaction zone is $(2V/R)(\bar{h}/2) = V\bar{h}/R$, i.e., the product of the wall shear rate ($\gamma = 2V/R$) and the average distance ($\bar{h}/2$) of a point in the reaction zone from the wall. The average distance that a particle, starting somewhere in the reaction zone, would have to be carried to leave the downstream end of the reaction zone is $L/2$, and traveling at the above velocity, this distance would be covered in time $t = RL/2V\bar{h}$. During this time period, the typical distance that the particle would diffuse laterally is $\sqrt{2Dt}$, and we take this distance to be the effective width W_{ec} of the endothelial zone. Using the formula given above for \bar{h} , we find that

$$W_{ec} = \sqrt{4/3} \left(\frac{RLD}{V} \right)^{1/3}. \quad (6.1)$$

The volume of the endothelial zone is then $V_{ec} = \bar{h}LW_{ec}$. Letting c_{ec} denote the concentration of a chemical species in the endothelial zone and c its concentration in the reaction zone, diffusion between the zones changes the amount of the chemical above the endothelial cells at a rate given by Fick's law [17]:

$$V_{ec} \frac{dc_{ec}}{dt} = \bar{h}LD \frac{(c - c_{ec})}{\frac{1}{2} \left(\frac{W}{2} + W_{ec} \right)}. \quad (6.2)$$

Here, $\bar{h}L$ is the area of the interface between the zones, D is the diffusion coefficient, and the remaining term on the right side of the equation is the relevant concentration gradient. Rearranging this equation into the form

$$\frac{dc_{ec}}{dt} = k_{diff}(c - c_{ec}) \quad (6.3)$$

gives

$$k_{diff} = \frac{2D}{W_{ec} \left(\frac{W}{2} + W_{ec} \right)}. \quad (6.4)$$

Table 2 shows that k_{diff} increases as the flow velocity increases for fixed values of L , R , W , and D . This does not contradict the intuition that the effectiveness of transport between the two zones should decrease with increasing flow speed. We can see this by re-writing Eq (6.2) for the flux of molecules (number of moles per time unit) between the two zones using the formulas for \bar{h} and W_{ec} presented above:

$$V_{ec} \frac{dc_{ec}}{dt} = \left\{ \frac{\frac{3}{4} \left(\frac{RLD}{V} \right)^{1/3}}{\frac{1}{2}W + \sqrt{\frac{4}{3} \left(\frac{RLD}{V} \right)^{1/3}}} \right\} 2LD(c - c_{ec}). \quad (6.5)$$

Table 2. Values of W_{ec} , k_{diff} , k_{flow}^c and shear rate γ for various V with $D = 5(10)^{-7}$ cm²/s, $R = 100$ μ m, $L = 10$ μ m, and $W = 10$ μ m

V , cm/s	W_{ec} , μ m	k_{diff} , s ⁻¹	k_{flow}^c , s ⁻¹	γ , s ⁻¹
0.5	2.49	5.4	8.1	100
2.5	1.45	10.7	23.6	500
7.5	1.01	16.5	49.1	1,500

The factor within braces on the right-side of Eq (6.5) is a decreasing function of V , so the total flux across the interface between the zones would decrease with V even for a fixed concentration difference $c - c_{ec}$; it decreases more strongly than this suggests because the concentration difference itself also decreases with V .

Acknowledgments

The work of ALF was supported in part by NSF grant DMS: FRG-0139926 and NT was supported by an NSF IGERT grant DGE-0217424.

References

- Kuharsky AL, Fogelson AL: Surface-mediated control of blood coagulation: The role of binding site densities and platelet deposition. *Biophys J* 2001;80:1050–1074.
- van't Veer C, Mann KG: Regulation of Tissue Factor initiated thrombin generation by the stoichiometric inhibitors Tissue Factor Pathway Inhibitor, antithrombin-III, and heparin cofactor-II. *J Biol Chem* 1997;272:4367–4377.
- Hathcock J, Menerson Y: Platelet deposition inhibits tissue factor activity: In vitro clots are impermeable to Factor Xa. *Blood* 2004;104:123–127.
- Esmon CT: The roles of Protein C and Thrombomodulin in the regulation of blood coagulation. *J Biol Chem* 1989;264:4743–4746.
- Broze GJ, Girard TJ, Novotny WF: Regulation of coagulation by multi-valent Kunitz-type inhibitor. *Biochem* 1990;29:7539–7546.
- Baugh RJ, Broze GJ, Krishnaswamy S: Regulation of extrinsic pathway Factor Xa formation by Tissue Factor Pathway Inhibitor. *J Biol Chem* 1998;273:4378–4386.
- Hindmarsh AC: ODEPACK, A systematized collection of ODE solvers; in Stepleman RS (ed): *Scientific Computing, IMACS Transactions on Scientific Computation*, Amsterdam, 1983, vol 1, pp 55–64.
- Turitto VT, Weiss HJ, Baumgartner HR: The effect of shear rate on platelet interaction with subendothelium exposed to citrated human blood. *Microvasc Res* 1980;19:352–365.
- Griffin JH: Control of coagulation reactions; in Beutler E, Coller B, Lichtman M, Kipps T, Seligsohn U (ed): *Williams Hematology*, New York, McGraw Hill, 2001, pp 1435–1447.
- Mann KG, Nesheim ME, Church WR, Haley P, Krishnaswamy S: Surface-dependent reactions of the vitamin K-dependent enzyme complexes. *Blood* 1990;76:1–16.
- Hockin MF, Jones KC, Everse SJ, Mann KG: A model for the stoichiometric regulation of blood coagulation. *J Biol Chem* 2002;277:18322–18333.
- Oliver JA, Monroe DM, Church RC, Roberts HR, Hoffman M: Activated protein C cleaves factor Va more efficiently on endothelium than on platelet surfaces. *Blood* 2002;100:539–546.
- Hoffman M, Monroe DM, Oliver JA, Roberts HR: Factors IXa- and Xa play distinct roles in tissue factor-dependent initiation of coagulation. *Blood* 1995;86:1794–1801.
- Hoffman M, Monroe DM: A cell-based model of hemostasis. *Thromb Haemost* 2001;85:958–965.
- Balasubramanian V, Vele O, Nemerson Y: Local shear conditions and platelet aggregates regulate the incorporation and activity of circulating tissue factor in ex-vivo thrombi. *Thromb Haemost* 2002;88:822–826.
- Nemerson Y, Turitto VT: The effect of flow on hemostasis and thrombosis. *Thromb Haemost* 1991;66:272–276.
- Keener J, Sneyd J: *Mathematical Physiology*. New York, Springer, 1998.
- Broze GJ, Miletich JP: Biochemistry and physiology of protein C, protein S, and thrombomodulin; in Colman RW, Hirsh J, Marder VJ, Salzman EW (ed): *Hemostasis and Thrombosis: Basic Principles and Clinical Practice*. Philadelphia, Lippincott, 1994, pp 259–276.